

Article

Synthesis of a Highly Efficient Mesoporous Green Catalyst from Waste Avocado Peels for Biodiesel Production from Used Cooking–Baobab Hybrid Oil

Anietie O. Etim ^{1,*} and Paul Musonge ^{2,3}¹ Department of Chemical Engineering, Durban University of Technology, Durban 4001, South Africa² Institute of Systems Science, Durban University of Technology, Durban 4001, South Africa; paulm@dut.ac.za³ Faculty of Engineering, Mangosuthu University of Technology, Umlazi 4031, South Africa

* Correspondence: anietie@dut.ac.za

Abstract: Valorization of waste biomass materials for fuels and other energy products has become one of the effective ways of escalating and improving the bioeconomy. The development of a novel biomass solid catalyst obtained from waste avocado peels and its potentials in transesterification of a bi-hybrid oil of used cooking–baobab oil (UC-BO) was investigated in this study. The catalyst was produced by calcining the burnt char of the dried avocado peels. The produced calcined avocado peels catalyst (CAP) was further characterized using analytical equipment, such as FT-IR, XRD, SEM, EDX, and TGA, to ascertain its catalytic properties. The results revealed that CAP contains some vital elements, such as Mg, P, Cl, Ca, Si, Na, and a high percentage of K content, present in form of oxides, carbonates, chlorides, and mixed metal compounds. The catalyst displayed effective catalytic potential in converting the UC-BO to biodiesel with 100% yield under an optimized condition of 51 min reaction time (RT), 14.5:1 of methanol to oil ratio (MTOR), and 2.73 wt% of catalyst loading (CL) at a constant temperature of 60 °C. The CAP exhibited excellent recyclability potential, achieving 92.85% biodiesel yield after five successive reaction cycles without notable catalytic activity reduction. The fuel properties investigated were all established within the biodiesel quality specifications of EN 14241 and ASTM D6751, demonstrating that it is a practical substitute for petroleum fuel.



Citation: Etim, A.O.; Musonge, P. Synthesis of a Highly Efficient Mesoporous Green Catalyst from Waste Avocado Peels for Biodiesel Production from Used Cooking–Baobab Hybrid Oil. *Catalysts* **2024**, *14*, 261. <https://doi.org/10.3390/catal14040261>

Academic Editor: Luigi Di Bitonto

Received: 13 March 2024

Revised: 29 March 2024

Accepted: 4 April 2024

Published: 15 April 2024



Copyright: © 2024 by the authors. Licensee MDPI, Basel, Switzerland. This article is an open access article distributed under the terms and conditions of the Creative Commons Attribution (CC BY) license (<https://creativecommons.org/licenses/by/4.0/>).

Keywords: avocado peels; biodiesel; green heterogeneous catalyst; optimization; transesterification

1. Introduction

The level of greenhouse gas emissions in the atmosphere has been recently reported to continue increasing due to the overconsumption of conventional fuels. The upfront effect of this is notable by the catastrophic environmental issues, such as climate change, global warming, depletion of the ozone layer, and toxic pollution, that threaten human health and bionetwork systems [1]. This situation will continue to deteriorate as the total primary energy consumption is presumed to increase by 57% by 2050 [2]. However, the utilization of bio-resources has attracted increasing attention from researchers and the government, due to their replenishing and sustainable nature in addition to the provision of enhanced CO₂ reduction and energy diversification to allow for a more secure and constant energy supply. This has consequently led to the energy switch from fossil fuels to low carbon resources, which creates a significant position for biomass energy. Among other renewable energy sources, biomass energy is the most widely utilized. Lignocellulosic biomass is the third-largest energy source after petroleum and coal products [3]. It contributes to the largest share of the renewable energy consumption in the form of bioenergy, with an estimated fast growing rate of 50% in the near future [4]. Its availability across the world makes it a desirable candidate for biofuel production. Biodiesel as one of the prominent biomass fuels is a domestic, clean-combusting, renewable fuel surrogate for fossil diesel. Biodiesel that is utilized as automobile fuel provides safety benefits alongside an increase in energy

security, air quality, and environmental improvement. The utilization of pure or unblended biodiesel is significantly harmless as compared to petro-diesel if spilled or released into the environment. According to ASTM specifications, biodiesel is less combustible and safer to handle and store due to a high flashpoint of greater than 130 °C, compared to the low flashpoint of 52 °C for fossil diesel [5].

Biodiesel is a diesel equivalent fuel, which is described according to the ASTM International standard as mono-alkyl long-chain esters of fatty acids obtained from bio-lipids.

Sustainable development for alternative energy requires the availability of potential feedstock for future applications. Biological feedstock for the production of biodiesel includes non-edible and edible oils, used oils, and algae. While algae oil is expensive to obtain, edible oils are not sustainable due to the food vs energy conflict. Using waste and non-edible feedstock oils for biodiesel synthesis is an attractive solution to the feedstock crisis, as they are not competing with food sources. Waste cooking oil has been considered one of the cheapest and effective feedstock oils for biodiesel production [6]. It is abundantly available and can easily be obtained from local restaurants or shops at a minimal cost, if not completely free. It is usually discarded into local drainage after repeated cycles of frying; however, this method of disposal causes pollution of drainage systems and water bodies. Its utilization for biodiesel production could serve a dual advantage, which includes reduction of environmental pollution and biodiesel cost. On the other hand, underutilized plant oils, such as baobab kernel oil, with an oil content range of 30–68%, has been reported to be rich in monosaturated fatty acid and is widely applied in traditional medicine and cosmetic industries [7,8]. Its utilization for biodiesel production has not been widely studied. However, oil mixtures in biodiesel production ensure constant feedstock supply and optimization as well as improvement of fuel properties [9].

Among the various techniques used in oil conversion to biodiesel, catalytic transesterification is the simplest and most economical method used for biodiesel production [10]. The triglycerides transesterification requires alcohol (usually methanol or ethanol as the short chain alcohol) and effective catalysts. Several catalysts, such as enzymes, and homogeneous and heterogeneous catalysts, have been reported to be effective for this process. However, homogenous- and enzyme-catalyzed transesterification suffer various drawbacks ranging from toxic waste generation and complicated separation of the homogeneous catalyst from the mixture during extraction to high cost and slow reaction of the enzyme [10–12]. Heterogeneous catalysts overcome these limitations and become the most preferred choice due to their easy recoverability, reusability, and non-corrosive characteristics [13]. The popularity of heterogenous catalysts became much stronger in recent research on biodiesel production because it can be derived from agricultural waste materials. This is due to their mineral-rich contents, which are the requisite ingredients for heterogeneous catalyst development. Agro-waste catalysts possess good catalytic properties, in addition to their availability, eco-friendliness, and cost effectiveness in their process synthesis. Agricultural materials recently investigated for heterogenous catalysts with promising catalytic activities included the following: pomelo leaves [14], the peels and trunk of *Musa acuminata* [15,16], *Heteropanax fragrans* [7], Radish leaves [17], Tucuma peels [18], *Musa paradisiaca* peels [19], moringa leaves [20], *Brassica nigra* [21], and red banana peduncle [22].

The avocado plant (*Persea Americana*) is a popular tree from the family of the *Lauraceae* species. It is a medium-sized tree and native to South Central Mexico and Guatemala. It thrives well in tropical and Mediterranean climates [23]. The fruits have smooth, buttery, golden-green flesh when ripe. Furthermore, the fruits contain high bioactive compounds like vitamin C, B, and E, unsaturated fatty acids, lutein, dietary fiber, pigment and phenolic compounds, and are majorly consumed globally because of its health benefits [24]. According to the food and agriculture organization (FAO) corporate statistics, the estimated total global production of avocado in 2021 was 8,685,672 metric tons, about a 7.2% increase as compared to 2020 with 8104.028 tons. Mexico was the largest with over 28% of the global production. Figure 1a,b show the list of countries by avocado production from 2016 to 2021, while Figure 1b, shows the avocado production by region in South Africa. Avocados

are largely produced in three provinces in South Africa, including Limpopo with 54% production, followed by Mpumalanga with 22%, and KwaZulu Natal with 18%. Avocado is a popular fruit that is mainly consumed in fresh and processed forms. According to [25], the present market growth of avocado fruits is expected to double by 2024. With this large increase, there is a great concern over the waste disposal of its peels, which are the major byproduct and constitutes 13–14% of the fruit weight [26]. Avocado peels have less economic value compared to its fruit and seeds. It is reported that it has been used for animal feed and as preservatives in the food industry [23,26]. However, the descriptive analysis of its raw peels revealed that it contains important minerals and elements, such as potassium (485 mg/kg), phosphorus (52 mg/kg), magnesium (29 mg/kg), calcium (12 mg/kg), sodium (7 mg/kg), and others such as manganese, iron, and zinc, which are less than 1 mg/kg [23,25]. The presence of the basic ingredients for a heterogeneous catalyst, such as high potassium content and other key elements, suggest that it could be deployed to serve as a viable biomass catalyst for biodiesel synthesis. However, to the best of our knowledge, the catalytic application of avocado peels as a catalyst for transesterification has not been studied or reported.

Hence, this study seeks to explore the process behind the synthesis and application of avocado peels as a heterogeneous catalyst for the production of optimized biodiesel from waste cooking–baobab hybrid oil, which is the novelty of this investigation. The influential parameters affecting the transesterification of the process, such as the methanol to molar oil ratio and process reaction time, were optimized and statistically analyzed by the response surface methodology-Box–Behnken design (RSM-BBD) model, while the reaction temperature of 60 °C was held constant throughout the experiment. The characterization and recyclability of the synthesized catalyst were also investigated and presented. Thus, this study adds an advantage to the bio-refinery exploration of sustainable resources with the overall impact of achieving a cost-effective biodiesel production process.

(a)

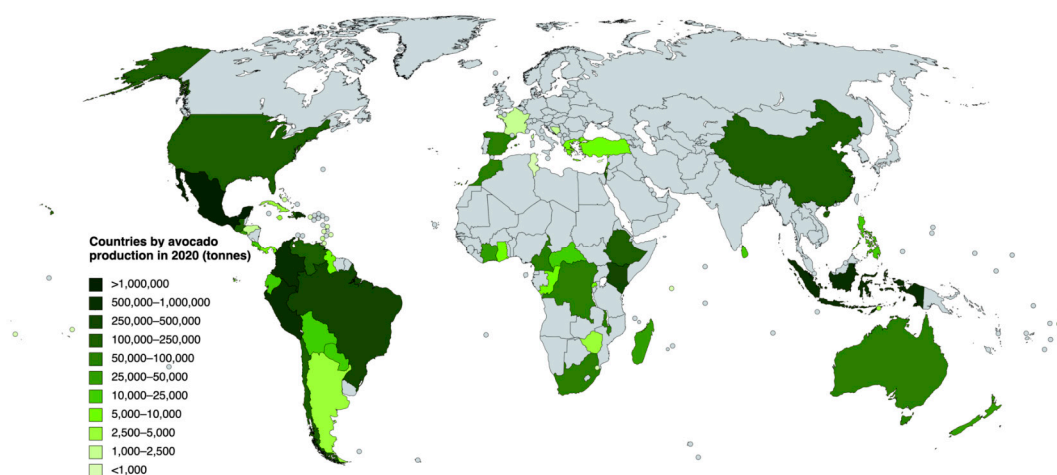


Figure 1. Cont.

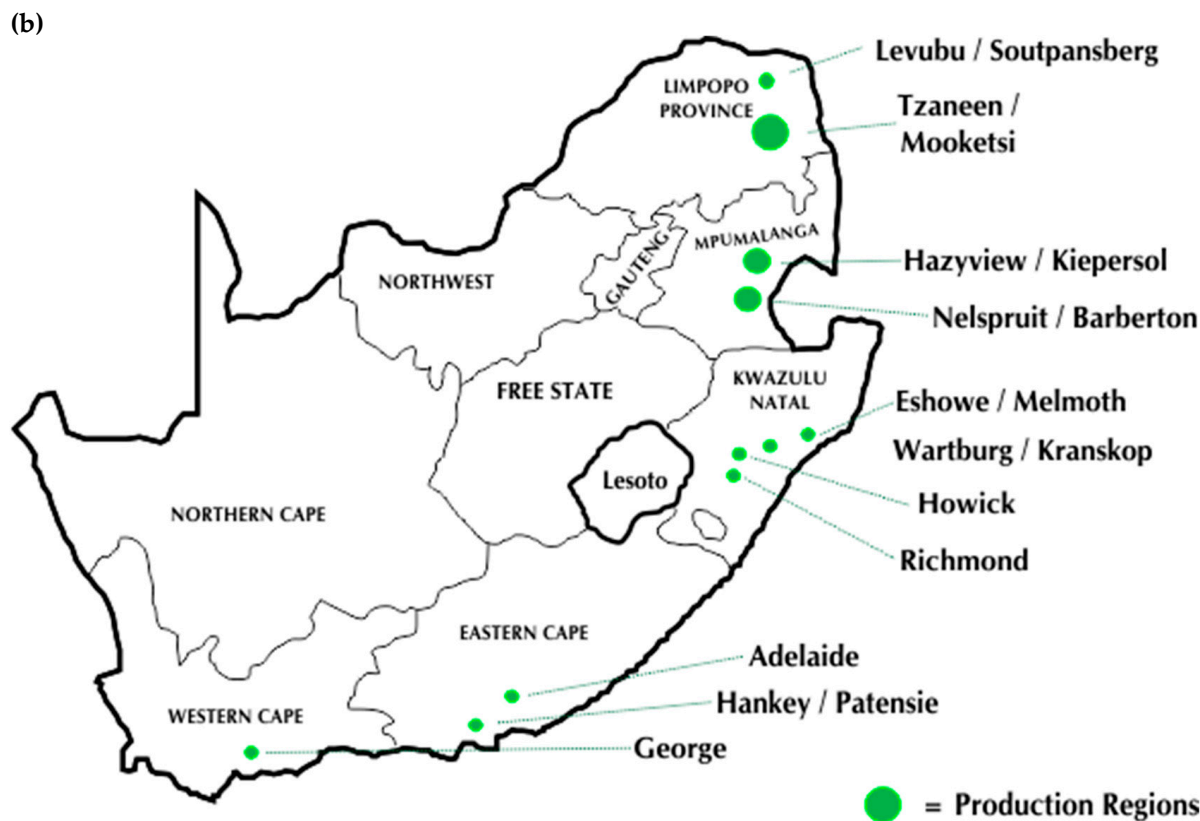


Figure 1. (a) Avocado production by country and (b) avocado production by region in South Africa.

2. Results and Discussion

2.1. CAP Catalyst Characterization

FT-IR Analysis

FT-IR spectroscopy was used to determine the functional group band vibrations of the generated catalyst. As displayed in Figure 2a–c, the IR spectra of the raw avocado peels (RAP), open-air burnt avocado peels (BAP), and calcined avocado peels (CAP) at 650 °C revealed several adsorption vibrations. The spectra provide morphological details about a certain vibration band that distinctively characterizes a particular functional group present in the sample. The stretching vibrations of O-H and K-O were, respectively, attributed to the bands at 3300 and 600 cm^{-1} [17]. The existence of carbonate compounds like K_2CO_3 is indicated by the absorption band at around 1600, 1300, and 1000 cm^{-1} , which are attributed to the asymmetric stretching of the carbonates functional group, and bending vibration of the C-O group [21,27]. Due to the high heat treatment, the K_2CO_3 bands at around 1300 and 1000 cm^{-1} are conspicuous and more prominent in the CAP spectrum than in the BAP and AP spectrums. The adsorption band around 1400 cm^{-1} can be attributed to the adsorbed atmospheric CO_2 on the metal oxide [28,29]. The band at 800 cm^{-1} found in the CAP spectra can be accredited to the Si-O-Si vibration, which is common in calcined agricultural waste materials [11,30]. The band at 600 cm^{-1} is attributed to the K-O and Ca-O stretching vibrations, suggesting the presence of CaO and K_2O in CAP (Gohain et al., 2020). The N-K-O bonds (where N = P or Mg) may be associated with the adsorption band located around 2900 and 1800 cm^{-1} [29]. The results in this section are also supported by the EDS analysis.

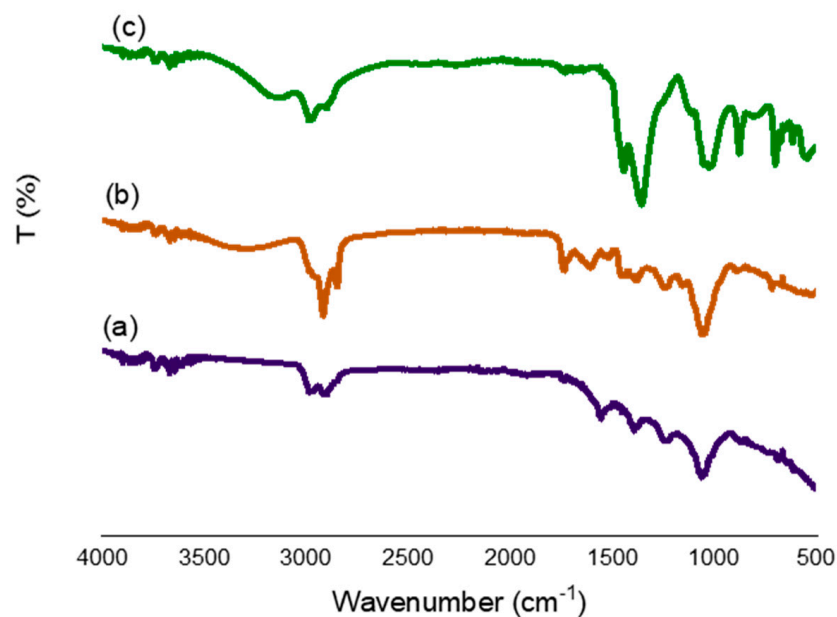


Figure 2. IR spectra of (a) raw avocado peel (RAP), (b) burnt Avocado peels (BAP), and (c) calcined avocado peels (CAP) samples.

2.2. XRD Analysis

The presence of crystalline molecules in BAP and CAP was determined using the XRD analysis (Figure 3). The existence of the metals and compounds in the catalyst, including potassium, magnesium, and calcium compounds, in carbonate, oxide, chloride, and silicate forms, are illustrated in Figure 3a,b. The diffraction peaks were observed to be more intense in the CAP spectrum than the BAP due to high heat of calcination. The strong peak diffraction of K compounds was noticed after calcination in CAP, which is in corroboration with the dominant K_2CO_3 bands in the FTIR spectra of CAP and the high percentage fraction of K in the EDX analysis. This observation was also reported in the characterization of cocoa pod husks and banana peels [22,27]. The strong characteristic diffraction peaks indicating the presence of KCl were observed at $2\theta = 28, 40, 48, 58, 65$, and the peaks diffraction observed at $2\theta = 12, 25, 30$, and 32 were due to K_2CO_3 , while $2\theta = 45$ and 62 were due to existence of MgO. The existence of other small diffraction peaks corresponding to $Ca_2Al_2(SiO_4)_2$, $CaK_2H(PO_4)_2$ and $K_2Al_2Si_2O_{10}$ as also observed. Using Scherrer's equation, which is provided in Equation (1), the average crystallite size was determined to be 46.30 nm. EDX and FTIR, which showed a high dispersal of K, Mg, P, Ca, and Si, substantially support the XRD results. The result is consistent with other heat-treated agricultural waste chars reported in the literature, including chars made from Tucuma peels [18], moringa leaves [20], pineapple leaves [31], *Musa acuminata*, and so forth.

$$D = \frac{\kappa\lambda}{\beta\cos\theta} \quad (1)$$

where D stands for Crystallite size (nm)

K represents Scherrer's constant denoted by (K = 0.9)

λ represents X-ray wavelength equal to 0.15406 (nm)

β represent the Radian for full width at half maximum (FWHM)

θ represents the Bragg-diffraction angle (Peaks position) in radians.

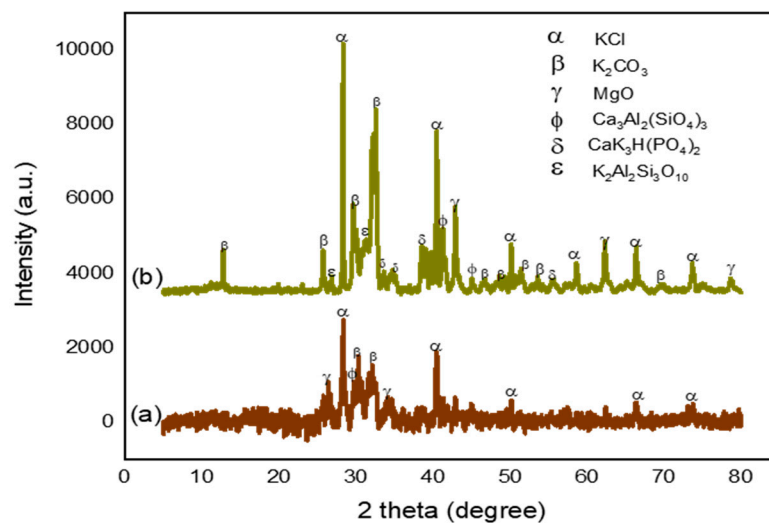


Figure 3. XRD spectra of (a) Burnt avocado peels (BAP), and (b) calcined avocado peels (CAP).

EDS Analysis

The elemental composition of raw, dried, and calcined avocado fruit peels that were calcined at 650 °C was determined using the EDS analysis. The elements obtained and their percentage and fractions are presented in Table 1. It is apparent from the table that certain elements increase and decrease due to the effect of the calcination process. The EDX result reveals that the calcination process is efficient in extracting and successfully improving available minerals present in the avocado peels. The observed element compositions are clearly in congruence with the XRD analysis outcome. The percentage of carbon in the raw and burnt avocado peels were found to be 64.52% and 49.95%, respectively. The fraction was found to decrease significantly in the calcined avocado peels ash due to the formation of carbonates and oxides, while other elements were observed to improve alongside the formation of new ones at higher heat treatment. The elements in CAP are arranged in the following sequence of increasing mass: K > P > Mg > Cl > Ca > Na > S > Si, with K being the greatest. The XRD, where K was exhibited the most, and the EDX results are consistent. Hence, CAP has a variety of mineral oxides and chlorides, the most important of which are KCl, K₂O, and MgO. These elements provide CAP with high catalytic activity in the bi-hybrid oil transesterification reaction. Other agro-waste catalysts which used to produce biodiesel have been found to include similar mineral compounds, with K being the greatest [17,32,33].

Table 1. Composition of elements of raw, burnt, and calcined avocado peels.

Heat Treatment Condition	Composition (%)									
	C	O	Na	Mg	Si	P	S	Cl	K	Ca
CAP at 650 °C, 3 h	7.20	36.71	0.4	2.54	0.41	4.17	0.46	1.84	45.0	1.65
Burnt AP	49.95	30.78	-	1.20	0.16	1.85	0.21	0.75	14.30	0.80
Raw AP	64.52	24.50	-	0.86	-	0.43	0.16	-	9.26	0.27

2.3. SEM Analysis

The SEM technique was used to examine the structural images of the green-based catalyst obtained from avocado peels. The images were taken at a magnitude of 1000× and are displayed in Figure 4a–c. The figure revealed the morphological transformation of RAP, BAP, and CAP based on their different levels of thermal treatment. Figure 4a shows the microporous structure and spongy nature of the raw avocado peels (RAP), while in Figure 4b, the open-air burnt (BAP) sample revealed the aggregate of irregular particle size and the spongy-like nature of the catalyst structure. The calcined (CPA) samples

(Figure 4c) revealed the fibrous, spongy, and mesoporous features of the catalyst with increased porosity. The high temperature of calcination resulted in the sintering of the mineral particles. Thus, the agglomeration and shiny appearance of the particles in CAP might be due to the presence of oxygenated materials, such as carbonates and oxides of various metals [11]. This is also in support of the XRD and FTIR analysis results. However, the higher temperature of calcination also favored the uniform distribution of the catalyst and elimination of organic elements present in the waste avocado peels [27]. The increase in the porosity of CAP enhanced significant activity that resulted in the high yield of FAME. Similar reports and morphological changes were also observed and reported on for various lignocellulose agro-biomass residues, such as pineapple leaves, cocoa pod, banana peduncle, *Carica papaya* stem and peels, and kola nut husks [17,30,32].

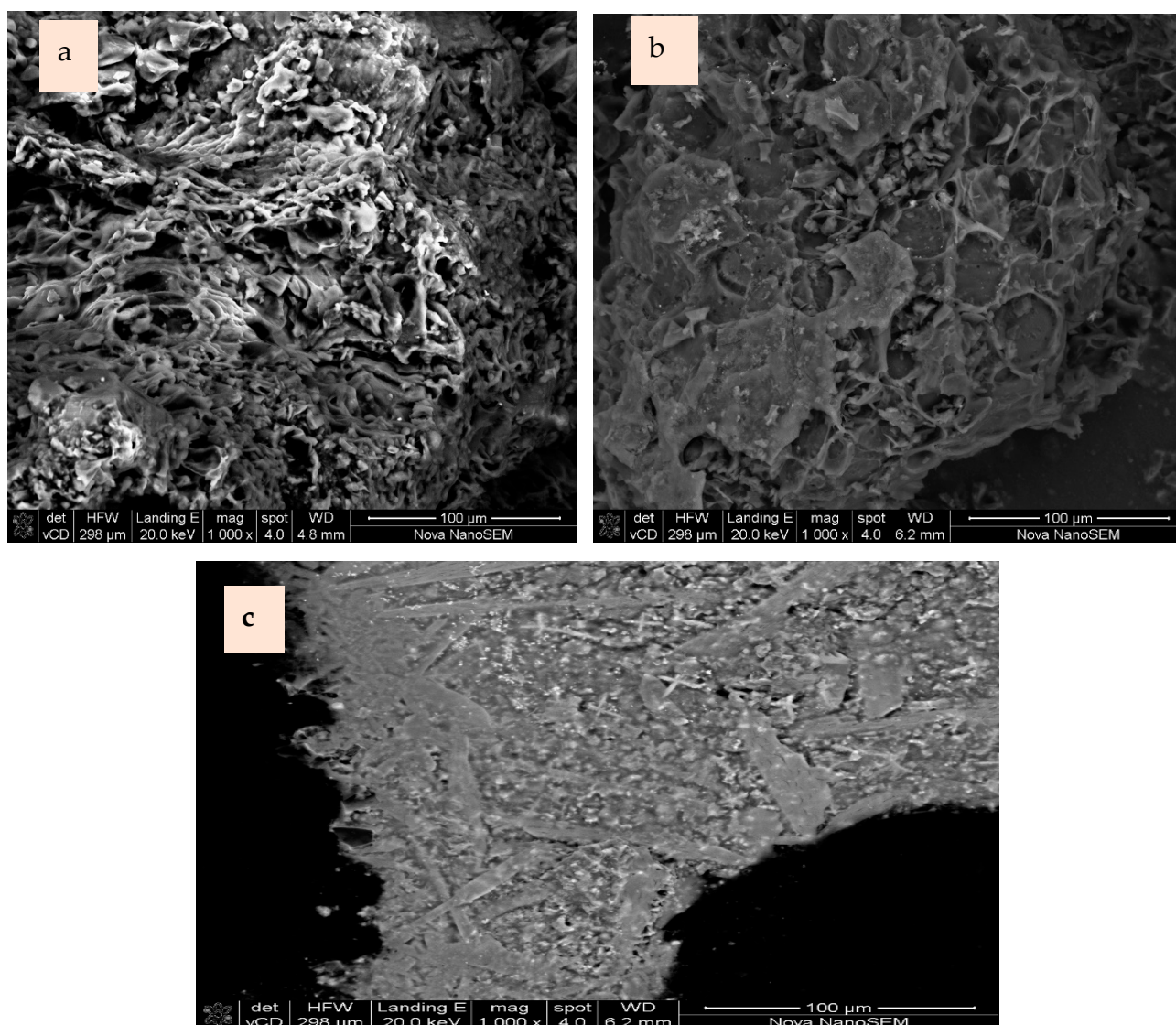


Figure 4. SEM images of (a) RAP, (b) BAP, and (c) CAP.

2.4. The Thermogravimetric Analysis (TGA)

The TGA results of the CAP catalyst and the percentage of weight loss as a function of temperature are displayed in Figure 5. The results indicate that the mass losses occurred gradually. The initial 4% weight loss that occurred between 85 and 150 °C could be assigned to the loss of moisture that had been adsorbed and chemisorbed [14]. The second stage of weight loss of 2.0% occurred between 180 and 580 °C and corresponded to the structural loss, which could be attributed to cracking, de-polymerization, hemicellulose, and decar-

boxylation of cellulose, leading to the release of volatile and non-volatile gases [17]. The changes at the ash phase, with the weight loss of 6.0%, occurred between 580–800 °C. These changes may be attributed to the dihydroxylation of OH units of the CAP catalyst, the loss of H₂O, and emission of CO₂, CO, etc., resulting from the oxidation of carbonaceous materials present in the catalyst. This leads to the breakdown of metal carbonates, such as K₂CO₃, into its corresponding oxide, K₂O, which is considered an active component of the agro-waste heterogeneous catalysts [22]. Calcination at high temperature improves the mineral content in organic materials, enhances the reusability and reduces leaching rate of the catalyst when used in the transesterification process.

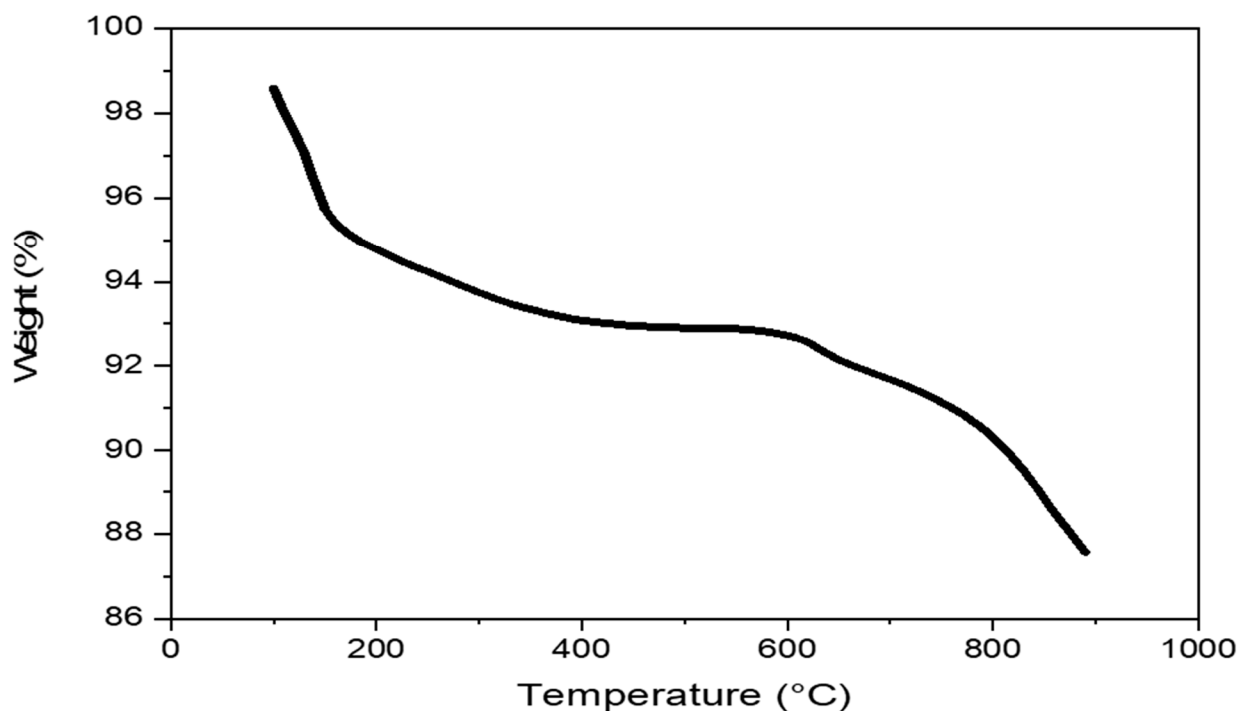


Figure 5. The TGA of calcined avocado peels.

2.5. Modeling and Optimization Results

The transesterification process was modeled using BBD with three level three components, comprising 17 experimental runs. The results show that the FAME yield vary between 79 and 99.98 wt%, and the regression multiple analysis of the polynomial second order equation, which describes the transesterification reaction process for FAME yield, is as follows:

$$Y = 95.72 - 4.50K_1 + 6.30K_2 - 1.73K_3 + 0.58K_1K_2 - 0.22K_1K_3 + 1.72K_2K_3 - 2.40K_1^2 - 3.25K_2^2 - 0.54K_3^2 \quad (2)$$

The result of the analysis of regression (ANOVA) is given in Table 2. The linear terms (K_1 , K_2 , K_3), the quadratic terms (K_1^2 , K_2^2 and K_3^2) and two of the cross products (K_1K_2 and K_2K_3) are all significant at $p < 0.5$, each with a significantly low p -value of $p < 0.0001$. The sum of squares value of 591.97, high F -value of 405.06, and $p < 0.0001$ all confirm the model effectiveness and show a good analysis of regression [34]. The model accuracy and reliability were statistically juxtaposed using R^2 , R , adjusted R^2 , MAE and AAD. The obtained $R^2 = 0.9981$ indicates that the observed data is properly aligned to the model regression equation. The adjusted $R^2 = 0.9960$ indicates the model significance and accurate estimation of the model. The predicted $R^2 = 0.9812$, adequate precession (69.86), low values of mean absolute error (MAE) of 0.02%, absolute average deviation (AAD) of 0.001%, and insignificant lack of fit all establish the significance and accuracy of the developed model. The graph of actual versus predicted biodiesel yield is shown in Figure 6a, which is also

in support of the model analysis. The outlier plot for all the experimental conditions is displayed in Figure 6b,c. All the studentized residuals were within the limit interval of ± 4.0 , illustrating the model significance. Figure 6d illustrates the selection of an adequate exponent (Lambda = 1) to normalize the data due to residual error. On the other hand, the lambda values ranging from -5 to $+5$ suggest that the transformed data have the highest likelihood of being normal data. Therefore, the lambda values obtained and the best lambda of -0.81 show that the data were normal and supported by the polynomial model, which was chosen for its accuracy [35].

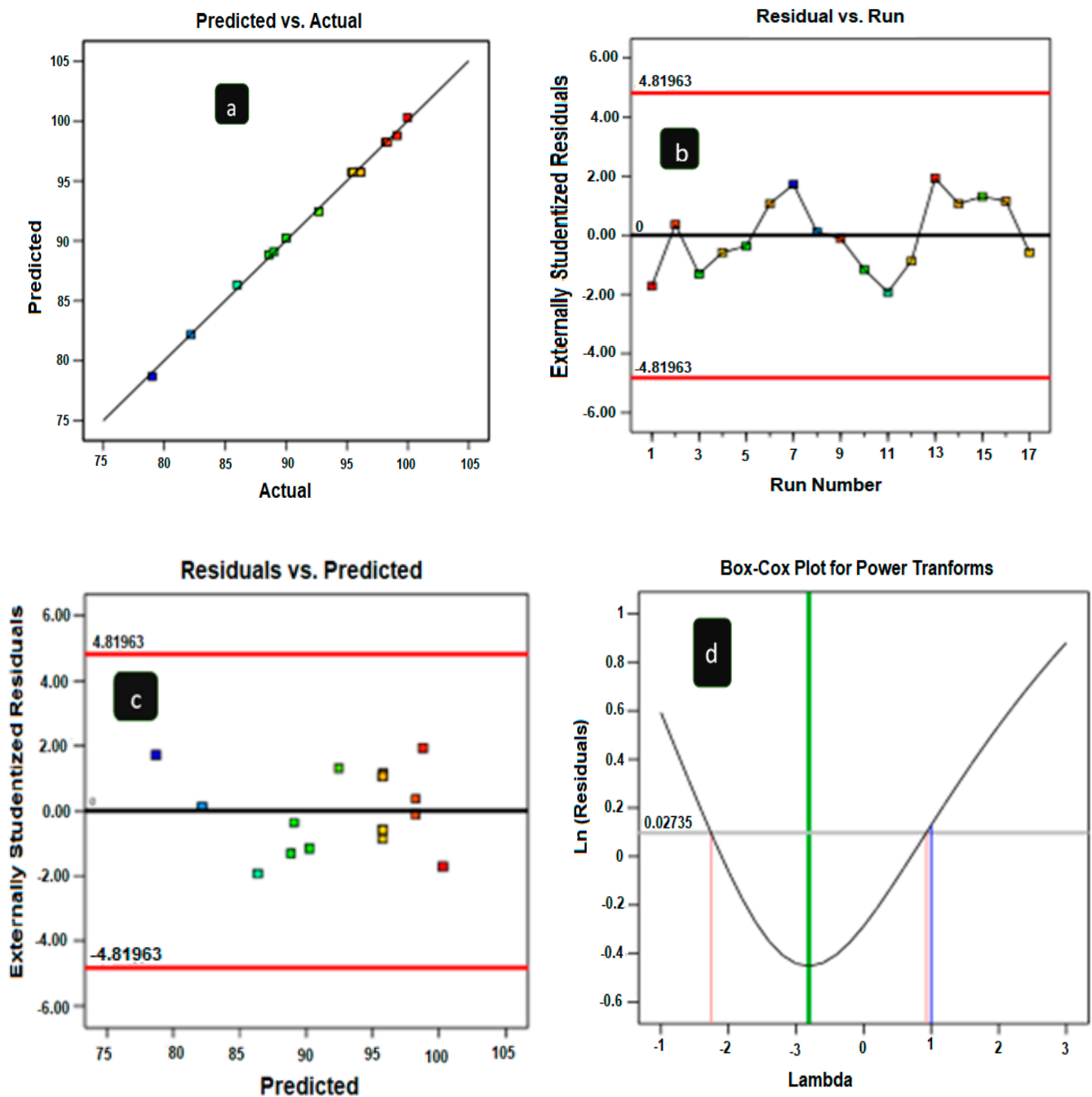


Figure 6. Diagnostic plots of the FAMEs produced by CAP.

Table 2. The test for significance through ANOVA for model and parameters.

Source	Coefficient Estimate	Sum of Squares	df	Mean Square	F-Value	p-Value
Model	95.72	591.97	9	65.77	405.06	<0.0001
K ₁ -Catalyst concentration	−4.50	161.91	1	161.91	997.09	<0.0001
K ₂ -Methanol/oil	6.30	317.27	1	317.27	1953.84	<0.0001
K ₃ -Reaction Time	−1.73	23.84	1	23.84	146.81	<0.0001
K ₁ K ₂	0.5800	1.35	1	1.35	8.29	0.0237
K ₁ K ₃	−0.2225	0.198	1	0.198	1.22	0.3060
K ₂ K ₃	1.72	11.90	1	11.90	73.30	<0.0001
K ₁ ²	−2.40	24.23	1	24.23	149.20	<0.0001
K ₂ ²	−3.25	44.51	1	44.51	274.09	<0.0001
K ₃ ²	−0.5437	1.24	1	1.24	7.67	0.0277
Residual		1.14	7	0.16		
Lack of Fit		0.648	3	0.22	1.77	0.291
Pure Error		0.488	4	0.12		
Cor Total		593.11	16			
Fit Statistic of the model						
R ²		0.9981		R	0.9990	
Adjusted R ²		0.9963		MAE	0.020%	
Predicted R ²		0.9812		AAD	0.001%	
Adeq Precision		69.8648				

2.6. Effect of the Process Variables Interaction

Figure 7a–c shows a graphical representation of the regression equation used to optimize the UCO-BO bi-hybrid oil transesterification using CAP.

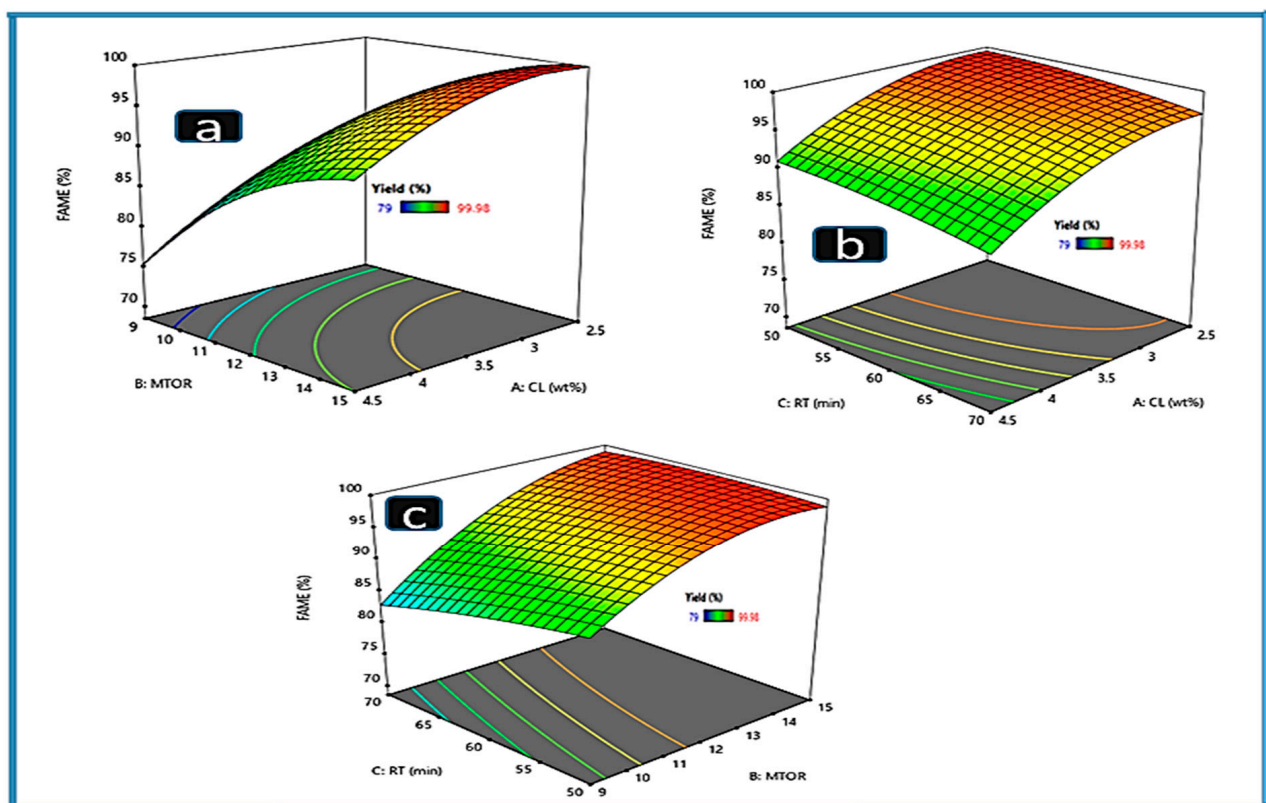
**Figure 7.** 3D surface plot of parameters' interaction.

Figure 7a shows the 3D response surface plot that illustrates the influence of the relationship between the methanol to oil molar ratio (MTOR) and catalyst loading (CL). One crucial factor influencing the transesterification reaction process is the ratio of methanol to oil. Methanol is needed for the reversible reaction of the transesterification process in order to boost the yield, beyond the theoretical stoichiometric ratio of 3:1. The transesterification reaction time was maintained at 60 min and 60 °C, while the MTOR was varied from 9:1 to 15:1 and the CL varied from 2.5 wt% to 4.5 wt%. FAME yield(s) was greatly increased by raising the MTOR levels and lowering the catalyst loading (CL) levels. Thus, this can be linked with the need for excess methanol to alter the equilibrium reaction in favor of the FAME yield. An increase in the FAMEs was observed to occur from CL of 2.5–3.5 wt% and MTOR of 10.5:1–15:1. A further increase in CL beyond 3.5 wt% and decrease in MTOR below 10:1 led to significant decrease in FAME yields. Table 2 indicates the significant effect of the mutual interaction of the two parameters (K_1K_2) with the $p < 0.023$ and F -value of 8.29. Similar trends have been reported on ash-based agro-waste heterogeneous catalysts obtained from the red banana peduncle (RBP), tucuma peels, and cocoa pod husks [18,27].

The relationship between reaction time (RT) and catalyst loading (CL) and the FAME yield at a fixed temperature of 65 °C and methanol ratio of 12:1 is displayed in Figure 7b. In the transesterification process, reaction time and catalysts are crucial variables, particularly when a heterogeneous catalyst is involved. In a heterogeneously catalyzed process, the mass transfer rate and catalyst presence have a significant impact on the reaction rate. Nevertheless, adequate time is required for the reactants to come into appropriate contact. Excessive reaction time can promote the backward reaction due to a loss of some volatile component of the reaction [36]. On the other hand, excessive catalyst loading may potentially make the mixture too viscous, which would impede the mass transfer process. The Figure indicates that FAME yield was at peak at low CL and RT. Table 2 shows that the mutual contact of these parameters (K_1K_3) was not significant with the p -value of 0.30 and F -value of 1.22. Nonetheless, the oil was converted to biodiesel within the range of time and catalyst values chosen for this experiment.

The effect of the interaction between the process reaction time (RT) and methanol to oil ratio (MTOR) at constant catalyst loading (CL) of 3.5 wt% is demonstrated in Figure 7c. An increase in FAME yield was noticed at low RT and high MTOR. The reaction time (RT) beyond 60 min results in a significant decrease in yield, which favors the backward direction of the equilibrium reaction of the transesterification process. The mutual interaction impact of both parameters (K_2K_3) in Table 2 indicates that they are very significant with the F -value of 73.30 and $p < 0.0001$. Thus, the selected range and levels of these parameters were sufficient for the process of hybrid oil conversion to biodiesel. To validate the model prediction for the maximum yield, the input process parameters were set in the range while the yield of biodiesel was set at maximum. The optimal conditions predicted were CL of 2.73 wt%, MTOR of 14.5:1, and RT of 51 min. Thus, a triplicate experiment was performed to verify the predicted condition and the biodiesel average yield of 100% was achieved. A similar yield of 100% was recorded by [37], when *Musa balbisiana colla* peels were employed to trans-esterify used cooking oil. Again, 99.93% yield was also reported when cocoa nut pod husks were used to trans-esterify neem oil [27] and several others.

2.7. Reusability Study of CAP

Reusability is an important characteristic of a heterogeneous catalyst when considering industrial upcycling. The test of reusability of CAP was studied under ideal conditions instituted by RSM. The recovered catalyst following the transesterification reaction was washed with hexane to remove agglomerated substances on the catalyst surface, and then placed in hot oven at 120 °C for 4 h. The dried catalyst was utilized in the subsequent reactions following the same conditions. CAP catalyst reusability test was repeated for up to five cycles with good catalytic activity and biodiesel yields. Figure 8 depicts the percentage of biodiesel yield(s) obtained after each cycle. It can be observed that the yields are minimally decreased after each cycle, which can be attributed to the gradual reduction

in the catalytic activity of CAP after each reaction cycle due to catalyst loss and leaching of the active metal during the recovery and separation process [3]. As shown in the EDX results, it is clearly indicated that potassium compound played a crucial role in the hybrid oil transesterification process, although other metals, such as Mg, P and Ca, also contribute to some extent to the strength of the catalytic activity of the developed catalyst. This is also in line with the reusability results reported with other biomass catalysts used in transesterification, such as ripe plantain peels [19], *Musa acuminata* trunk [16], and papaya stem [29].

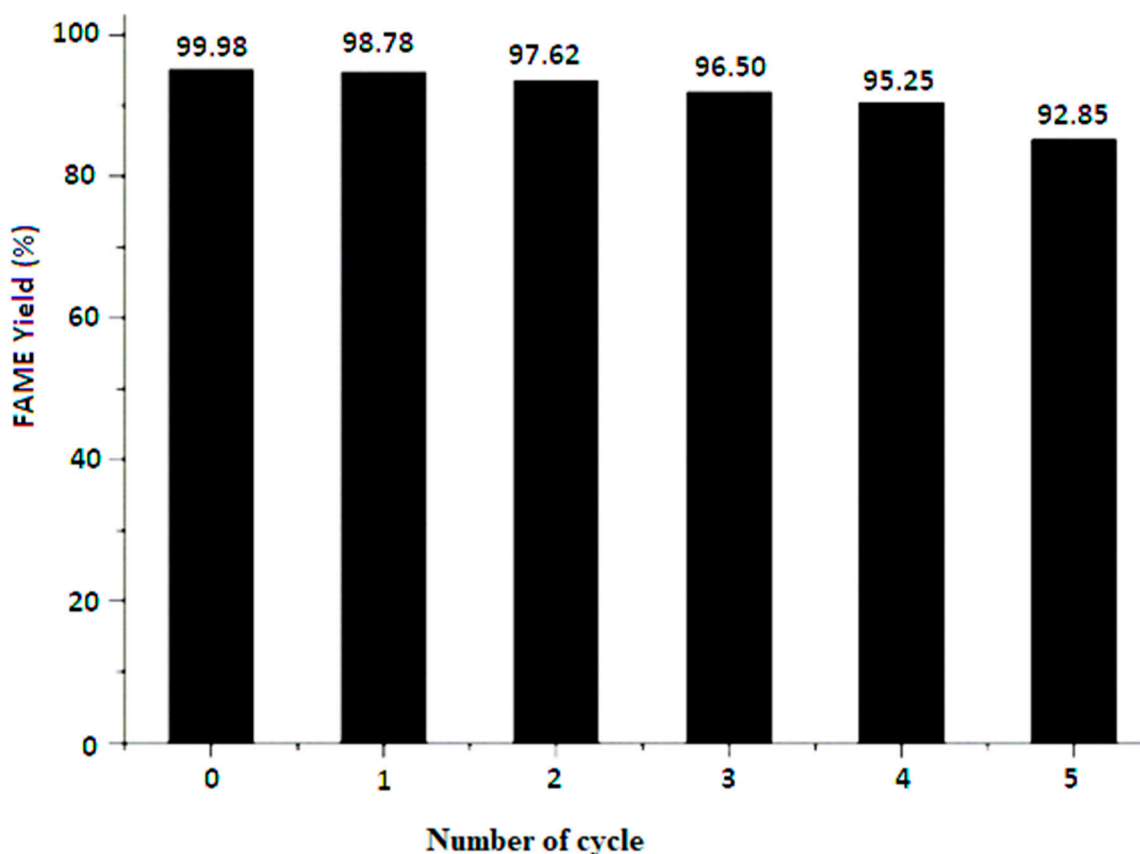


Figure 8. Reusability cycles of CAP catalyst.

2.8. Biodiesel Quality Characterization

Quality compositions of the developed biodiesel using CAP catalyst were established in accordance with the standard method of ASTM D6751 and EN 14214 [38]. The obtained results are depicted in Table 3 and indicate the properties which are well established within the biodiesel quality standard limits. The produced biodiesel has a density of 0.886 g/cm^3 at $15 \text{ }^\circ\text{C}$, which falls within the biodiesel standard specification. The obtained value indicates that the produced fuel will promote efficient combustion with reduced emission of toxic hydrocarbons [34]. The viscosity was established to be $3.20 \text{ mm}^2/\text{s}$, which is lower than EN14214 limit but fits well with the range limit of ASTM D6751. This shows that the produced biodiesel has the potential to flow easily when injected into the engine with fewer droplets, good fuel atomization, and increased efficiency of operation within the engine. The acid number was ascertained by ASTM D664 to be 0.28 mg KOH/g , which is lower than the specified maximum limits of 0.5 max . This indicates that the biodiesel fuel produced is less corrosive and will not damage the fuel supply systems of the engine [39]. The caloric value and the cetane number were determined to be 40.5 MJ/Kg and 60, respectively, which are higher than the specified minimum standard of ASTM D6751 and EN 14214. The obtained result for calorific value was found to be comparable with other biodiesel results as reported in the literature, $40.20, 39.60, 43.13 \text{ MJ/kg}$ [16,17],

and is higher than the minimum standard limits specified by ASTM D6751 and EN 14214. The results apparently show that the high thermal content of the produced FAMES will enhance the energy released during combustion as compared to petro-diesel as well as enhance the quality of the combustion when undergoing compression ignition [40]. The water content of the FAMES was obtained, which is within the standard range of 0.05%. This implies that the produced fuel is well dried and is free of water that would have promoted microbial growth, tank corrosion, hydrolysis, and emulsion formation when stored. The iodine value of 78 (gI²/100 g) obtained is lower than the maximum limits stipulated by the ASTM 6751, which implies that the biodiesel fuel produced will positively impact the engine operation as it has reduced engine deposits and increased lubrication quality due to the limited unsaturated fatty acids present in the fuel [41].

Table 3. Produced biodiesel quality in comparison with standards.

Property	Unit	Test Method [38]	Present Study	ASTM D6751	EN 14214
Moisture content	%	ASTM D2709	0.01	<0.05	0.050% max
Density	g/cm ³	ASTM D4052	0.886	0.85	0.86–0.90
Kinematic viscosity at 40 °C	mm ² /s	ASTM D 445	3.22	1.9–6.0	3.5–5.0
Acid value	Mg KOH/g	ASTM D 664	0.38	0.5 max	0.5 max
Iodine value		AOAC	78	120 max	N/S
Copper strip at 50 °C, 3 h	Rating	ASTM D130	1	No. 3 max	Class 1 min
Calorific value	MJ/Kg		40.5	N/S	35 min
Cetane number	-	ASTM D613	60	47 min	51 min
API	deg		28.20	36.95	N/S

3. Materials and Methodology

3.1. Materials

The avocado fruits (Hass species) were obtained from fruit vendors at the open market along Steve Biko Road, Durban. The used cooking oil was obtained from the snack shop on campus at Steve Biko, Durban University of Technology. The baobab oil and all the analytical grade chemical reagents used in this experiment, including phenolphthalein (indicator), methanol (98%), cyclohexane, ethanol (98%), hydrochloric acid, diethyl ether, Wij's solution, potassium hydroxide, were made available by Lichro Chemical and Lab. Supplies cc, Durban, South Africa.

3.2. CAP Catalyst Preparation

The fruit peels of ripe avocados were removed and washed several times with water to eradicate all the impurities adhered at the surface. The washed avocado peels were sun dried for one week, and then charred in open air to generate powder. It was then sieved mechanically to obtain the powder particle size of >0.5 mm, and then further calcined in a programmable muffle furnace at 650 °C for 3 h. The burnt and calcined avocado peel ashes were labeled BAP and CAP, respectively, and kept in an airtight container for further use.

Characterization of CAP Catalyst

The Quanta 200 Nova NanoSEM system equipped with a micro-analyzer was used to investigate the elemental compositions of the catalyst together with the surface structure of the RAV, BAP, and CAP catalyst. The crystalline compounds and diffraction patterns in BAP and CAP were analyzed using a D-8 Advance diffractometer equipped with radiation (Cu K α) at a 2 θ range of 10–80 °C. The catalysts' crystallite average size was examined by Dedye–Scherrer's equation. Fourier-transform infrared spectroscopy (FT-IR) analysis was carried out to determine the functional group of the calcined peel biochar using FT-IR equipment (Perkin Elmer spectrum 100, PerkinElmer, Waltham, MA, USA) and was recorded in a spectra range of 4000–400 cm⁻¹. The thermal stability of the catalyst was analyzed (Netzsch, TG 209 F1 Libra, Selb, Germany) under inert atmosphere, at a heating range of 100–800 °C and heating rate of 10 °C/min, using nitrogen gas.

3.3. Blend Preparation of Used Cooking Oil–Baobab Oil (UCO-BO) Hybrid

The hybrid oil was prepared by filtering the used cooking oil to remove impurities. Thereafter, an equal weight of the two oils (UCO/BO) at 1:1 *w/w* was measured into a glass beaker and mixed at 60 °C for 20 min to remove moisture and to obtain a homogenous solution. The hybrid oil was allowed to cool and the physico-chemical properties, including acid value, density, heating value, viscosity, cetane number, iodine value, and refractive index, were determined in accordance with the standard methods.

3.4. Statistical Analysis of the Transesterification Process

The obtained data from the transesterification of the UCO-BO bi-hybrid experiment were statistically analyzed using RSM-BBD. The process input parameters and their levels and ranges of investigation are shown in Table 4, which includes 50–70 (min) of the process reaction time, 2.5–4.5 (wt%) catalyst amount and 9:1–15:1 (*w/w*) methanol to oil ratio. The generated matrix of the regression model for data fittings is given in Table 5. Analysis of variance (ANOVA) considered at 95% confidence level was used to appraise the model significance. The statistical parameters such as determination of the coefficient R^2 , predicted R^2 , and lack of fit were evaluated to guarantee the fitness of the model developed. The adjustability of the model was evaluated by the regression parameters, while diagnostic plots were used to examine and explain the effect of the model fitness. The effect of the interaction between the process parameters and yield is described by the 3D plot. The correlation between the yield and the response variables is best expressed by the second order differential equation given in Equation (3).

$$Y = F_0 + \sum_{i=1}^n F_i k_i + \sum_{i=1}^n F_{ii} k_i^2 + \sum_{i=1}^{n-1} \sum_{j=2}^n F_{ij} k_i k_j + \zeta \quad (3)$$

where Y represents the biodiesel yield, while F_0 , F_i , F_{ii} , F_{ij} are the model regression coefficients, and $K_i K_j$ are the process factors, and ζ is the error differential. The model was also validated by performing experiments under an established statistically optimal condition predicted by the software. The actual FAME yields produced and the estimated yields from the developed model together with the viscosity of the biodiesel acquired from each experimental run are displayed in Table 5.

Table 4. Operational levels and range of the factors.

Factors	Symbol	Unit	Levels and Coded Factor		
			−1	0	1
Catalyst loading	K_1	wt%	2.5	3.5	4.5
Methanol/oil molar ratio	K_2	<i>w/w</i>	9:1	12:1	15:1
Reaction time	K_3	min	50	60	70

Table 5. Empirical settings with actual and predicted yields, with their corresponding viscosity.

Std Order	Run	K_1 (wt%)	K_2 (<i>w/w</i>)	K_3 (min)	Yield (%)	Predicted Value (%)	Viscosity (mm ² /s)
3	1	2.5	15:1	60	99.98	99.97	2.99
12	2	3.5	15:1	70	98.30	98.22	2.84
1	3	2.5	9:1	60	88.60	88.85	2.52
14	4	3.5	12:1	60	95.50	95.72	3.11
9	5	3.5	9:1	50	89.00	89.08	3.27
15	6	3.5	12:1	60	96.10	95.72	3.10
2	7	4.5	9:1	60	79.00	78.69	3.50
11	8	3.5	9:1	70	82.20	82.18	2.94

Table 5. Cont.

Std Order	Run	K ₁ (wt%)	K ₂ (w/w)	K ₃ (min)	Yield (%)	Predicted Value (%)	Viscosity (mm ² /s)
10	9	3.5	15:1	50	98.20	98.22	2.85
6	10	4.5	12:1	50	90.00	90.23	3.72
8	11	4.5	12:1	70	86.00	86.33	3.15
13	12	3.5	12:1	60	95.40	95.72	3.01
5	13	2.5	12:1	50	99.11	98.78	3.18
17	14	3.5	12:1	60	96.10	95.72	3.29
4	15	4.5	15:1	60	92.70	92.45	3.16
7	16	2.5	12:1	70	96.00	95.77	2.86
16	17	3.5	12:1	60	95.50	95.72	2.87

Model Performance Evaluation

The model predictability efficiency of the transesterification response (yield) of the UCO-BO bi-hybrid oil was further evaluated using the statistical equations shown in Equations (4)–(7). The statistical parameters analyzed include coefficient correlation (R), determination coefficient (R^2), absolute average deviation (AAD), and mean absolute error (MAE).

$$\text{Correlation coefficient} \quad R = \frac{\sum_{i=1}^q (Z_{p,i} - Z_{p,m}) \cdot (Z_{a,i} - Z_{a,m})}{\sqrt{[\sum_{i=1}^q (Z_{p,i} - Z_{p,m})^2] [\sum_{i=1}^q (Z_{a,i} - Z_{a,m})^2]}} \quad (4)$$

$$\text{Coefficient of determination} \quad R^2 = 1 - \frac{\sum_{i=1}^q (Z_{a,i} - Z_{p,i})^2}{\sum_{i=1}^q (Z_{p,i} - Z_{a,m})^2} \quad (5)$$

$$\text{Average absolute deviation} \quad AAD = \frac{100}{q} \sum_{i=1}^q \left| \frac{Z_{a,i} - Z_{p,i}}{Z_{a,i}} \right| \quad (6)$$

$$\text{Mean absolute error} \quad MAE = \frac{1}{q} \sum_{i=1}^q \left| (Z_{a,i} - Z_{p,i}) \right| \quad (7)$$

where h , q , $Z_{a,i}$ and $Z_{p,i}$ represent input variables, experiment, and predicted values, respectively, while $Z_{a,m}$ denotes the experimental mean value, and $Z_{p,m}$ represents the predicted value.

3.5. Transesterification Reaction of UCO-BO Hybrid with CAP Catalyst

The major decisive factor of the transesterification step was the acid value and the corresponding FFA. The hybrid oil has an acid value of 4.25 (mg KOH/g) with a resultant %FFA of 2.13. Therefore, with the CAP catalyst, a single-step transesterification reaction process was used to convert the UCO-BO to biodiesel. The transesterification process of UCO-BO hybrid was executed in a 250 mL spherical bottom three-necked flask. The reactor was configured and fixed with some apparatus such as a reflux condenser to prevent the escape of some volatile component, or a reactant such as methanol, and a thermometer probe to monitor the temperature of the reactor content. A specific quantity of hybrid oil (30 g) was first measured and poured into the reactor, and then agitated on a magnetic hot plate set at 60 °C. The reactor content was let to heat to a required temperature, after which a measured quantity of methanol and CAP was added to the reactor according to the conditions of each experiment stipulated by the BBD in Table 5. To achieve homogeneity of the mixture, an agitation speed of 450 rpm was set and the reaction was allowed to run based on the time duration assigned for each experiment. The reaction mixture at the end was centrifuged at 1500 rpm for 5 min to remove the solids catalyst (used CAP) and the liquid part was transferred into a funnel for phase separation. The methyl ester layer was then washed with warm distilled water at 50 °C and heated to eradicate moisture. The recovered CAP was washed with hexane, and then dried at 120 °C for 4 h to be reused for subsequent experiments. To quantify the biodiesel obtained from each experiment, the yield was determined using Equation (8). The biodiesel produced was analyzed based on the ASTM D6751 methods. The mathematical expression used in determining the exact quantity of methanol utilized in the transesterification reaction process of the hybrid oil is given in Equation (9).

$$\text{Biodiesel yield (\%)} = \frac{\text{weight of obtained biodiesel (g)}}{\text{weight of oil sample used (g)}} \times 100 \quad (8)$$

$$Y(g) = \frac{W \times Q \times M}{Mw} \quad (9)$$

where Y is the alcohol weight, W is the hybrid oil weight, M is the molecular weight of alcohol, and Mw is the molecular weight of oil.

4. Conclusions

The present study investigates the production of a green heterogeneous catalyst from avocado peels and its efficacy in the transesterification of bi-hybrid oil of used cooking–baobab oil (UCO-BO) biodiesel. The study showed that the heterogeneous green catalyst generated from waste avocado peels has the potential to be a useful component in the transesterification process that produces biodiesel. The highest biodiesel yield of 100% was attained under the ideal conditions of catalyst loading of 2.73 wt%, molar ratio of methanol to oil 14.5:1, and reaction time of 51 min. The statistical assessment of the model significance, its predictability potential, and accuracy were indicated with the R (0.9999), R^2 (0.9998), and the adjusted R^2 (0.9996), with negligible error function of MAE (0.02%) and AAD (0.001%), respectively. The characterization results revealed that the synthesized catalyst was rich in potassium (K), while other metals such as Mg, Ca, P and Si were present in small quantities. The reusability investigations revealed that the avocado peel catalyst demonstrated excellent stability with the yield exceeding 92% after five rounds of reuse. The minimal deactivation noticed in the catalytic activity confirms the good thermal stability of the produced catalyst. The results of the fuel properties' characterization achieved in this study show that the synthesized biodiesel has suitable quality and is well established within the limit requirements for biodiesel. The developed catalyst is biodegradable in nature, nontoxic, environmentally friendly, thermally stable, reusable, available, cost effective, and efficient in oil conversion. Thus, CAP catalyst can be considered as a highly effective biomass-based catalyst for large-scale biodiesel production. Overall, the general protocol established can be adopted industrially for economical biodiesel production processes.

Author Contributions: A.O.E. Conceptualization, methodology, design, data collection and validation, investigation, formal analysis, writing—original draft. P.M.: Supervision, investigation, writing—review, funding acquisition. All authors have read and agreed to the published version of the manuscript.

Funding: This research received no external funding, and the APC was funded by the Durban University of Technology and Mangosuthu University of Technology and the Authors.

Data Availability Statement: The data presented in this study are available based on request because they were obtained from experimental work.

Acknowledgments: Authors appreciate the Durban University of Technology and Mangosuthu University of Technology for their financial support.

Conflicts of Interest: The authors declare no conflict of interest.

References

- Hajjari, M.; Tabatabaei, M.; Aghbashlo, M.; Ghanavati, H. A review on the prospects of sustainable biodiesel production: A global scenario with an emphasis on waste-oil biodiesel utilization. *Renew. Sustain. Energy Rev.* **2017**, *72*, 445–464. [[CrossRef](#)]
- Mansir, N.; Teo, S.H.; Rashid, U.; Saiman, M.I.; Tan, Y.P.; Alsultan, G.A.; Taufiq-Yap, Y.H. Modified waste eggshell derived bifunctional catalyst for biodiesel production from high FFA waste cooking oil. A review. *Renew. Sustain. Energy Rev.* **2018**, *82*, 3645–3655. [[CrossRef](#)]
- Al-mawali, K.S.; Osman, A.I.; Al-muhtaseb, A.H.; Mehta, N.; Jamil, F.; Mjalli, F.; Vakili-nezhaad, G.R.; Rooney, D.W. Life cycle assessment of biodiesel production utilising waste date seed oil and a novel magnetic catalyst: A circular bioeconomy approach. *Renew. Energy* **2021**, *170*, 832–846. [[CrossRef](#)]
- Wang, B.; Yang, Z.; Xuan, J.; Jiao, K. Crises and opportunities in terms of energy and AI technologies during the COVID-19 pandemic. *Energy AI* **2020**, *1*, 100–113. [[CrossRef](#)]

5. Knothe, G.; Razon, L.F. Biodiesel fuels. *Prog. Energy Combust. Sci.* **2017**, *58*, 36–59. [[CrossRef](#)]
6. Abdollahi Asl, M.; Tahvildari, K.; Bigdeli, T. Eco-friendly synthesis of biodiesel from WCO by using electrolysis technique with graphite electrodes. *Fuel* **2020**, *270*, 117–582. [[CrossRef](#)]
7. Modiba, E.; Osifo, P.; Rutto, H. Biodiesel production from baobab (*Adansonia digitata* L.) seed kernel oil and its fuel properties. *Ind. Crops Prod.* **2014**, *59*, 50–54. [[CrossRef](#)]
8. Msalilwa, U.L.; Makule, E.E.; Munishi, L.K.; Ndakidemi, P.A. Physicochemical Properties, Fatty Acid Composition, and the Effect of Heating on the Reduction of Cyclopropanoid Fatty Acids on Baobab (*Adansonia digitata* L.). *Crude Seed Oil* **2020**, *2020*, 669–1298. [[CrossRef](#)]
9. Giwa, S.; Adekomaya, O.; Nwaokocha, C. Potential hybrid feedstock for biodiesel production in the tropics. *Front. Energy* **2016**, *10*, 329–336. [[CrossRef](#)]
10. Osman, A.I.; Mehta, N.; Elgarahy, A.M.; Al, A.; Ala, H.; Al, H.; Rooney, D.W. Conversion of Biomass to Biofuels and Life Cycle Assessment: A Review. *Environ. Chem. Lett.* **2021**, *19*, 4075–4118. [[CrossRef](#)]
11. Basumatary, S.; Nath, B.; Das, B.; Kalita, P.; Basumatary, B. Utilization of renewable and sustainable basic heterogeneous catalyst from *Heteropanax fragrans* (Kesseru) for effective synthesis of biodiesel from *Jatropha curcas* oil. *Fuel* **2021**, *286*, 119–357. [[CrossRef](#)]
12. Gbadeyan, O.J.; Muthivhi, J.; Liganiso, L.Z.; Dziike, F. Recent improvements to ensure sustainability of biodiesel production. *Biofuels* **2024**, 1–15. [[CrossRef](#)]
13. Hashemzadeh Gargari, M.; Sadrameli, S.M. Investigating continuous biodiesel production from linseed oil in the presence of a Co-solvent and a heterogeneous based catalyst in a packed bed reactor. *Energy* **2018**, *148*, 888–895. [[CrossRef](#)]
14. Zhao, C.; Lv, P.; Yang, L.; Xing, S.; Luo, W.; Wang, Z. Biodiesel synthesis over biochar-based catalyst from biomass waste pomelo peel. *Energy Convers. Manag.* **2018**, *160*, 477–485. [[CrossRef](#)]
15. Pathak, G.; Das, D.; Rajkumari, K.; Rokhum, L. Exploiting waste: Towards a sustainable production of biodiesel using: *Musa acuminata* peel ash as a heterogeneous catalyst. *Green Chem.* **2018**, *20*, 2365–2373. [[CrossRef](#)]
16. Rajkumari, K.; Rokhum, L. A sustainable protocol for production of biodiesel by transesterification of soybean oil using banana trunk ash as a heterogeneous catalyst. *Biomass Convers. Biorefinery* **2020**, *10*, 839–848. [[CrossRef](#)]
17. Eldiehy, K.S.H.; Gohain, M.; Daimary, N.; Borah, D.; Mandal, M.; Deka, D. Radish (*Raphanus sativus* L.) leaves: A novel source for a highly efficient heterogeneous base catalyst for biodiesel production using waste soybean cooking oil and *Scenedesmus obliquus* oil. *Renew. Energy* **2022**, *191*, 888–901. [[CrossRef](#)]
18. Mendonça, I.M.; Paes, O.A.R.L.; Maia, P.J.S.; Souza, M.P.; Almeida, R.A.; Silva, C.C.; Duvoisin, S.; de Freitas, F.A. New heterogeneous catalyst for biodiesel production from waste tucumã peels (*Astrocaryum aculeatum* Meyer): Parameters optimization study. *Renew. Energy* **2019**, *130*, 103–110. [[CrossRef](#)]
19. Etim, A.; Betiku, E.; Ajala, S.; Olaniyi, P.; Ojumu, T. Potential of Ripe Plantain Fruit Peels as an Ecofriendly Catalyst for Biodiesel Synthesis: Optimization by Artificial Neural Network Integrated with Genetic Algorithm. *Sustainability* **2018**, *10*, 707. [[CrossRef](#)]
20. Aleman-Ramirez, J.L.; Moreira, J.; Torres-Arellano, S.; Longoria, A.; Okoye, P.U.; Sebastian, P.J. Preparation of a heterogeneous catalyst from moringa leaves as a sustainable precursor for biodiesel production. *Fuel* **2021**, *284*, 118–983. [[CrossRef](#)]
21. Nath, B.; Das, B.; Kalita, P.; Basumatary, S. Waste to value addition: Utilization of waste *Brassica nigra* plant derived novel green heterogeneous base catalyst for effective synthesis of biodiesel. *J. Clean. Prod.* **2019**, *239*, 118112. [[CrossRef](#)]
22. Balajii, M.; Niju, S. Banana peduncle—A green and renewable heterogeneous base catalyst for biodiesel production from *Ceiba pentandra* oil. *Renew. Energy* **2020**, *146*, 2255–2269. [[CrossRef](#)]
23. Figueroa, J.G.; Borrás-Linares, I.; Del Pino-García, R.; Curiel, J.A.; Lozano-Sánchez, J.; Segura-Carretero, A. Functional ingredient from avocado peel: Microwave-assisted extraction, characterization and potential applications for the food industry. *Food Chem.* **2021**, *352*, 129–300. [[CrossRef](#)]
24. Nyakang’i, C.O.; Ebere, R.; Marete, E.; Arimi, J.M. Avocado production in Kenya in relation to the world, Avocado by-products (seeds and peels) functionality and utilization in food products. *Appl. Food Res.* **2023**, *3*, 100–275. [[CrossRef](#)]
25. Ramos-Aguilar, A.L.; Ornelas-Paz, J.; Tapia-Vargas, L.M.; Gardea-Béjar, A.A.; Yahia, E.M.; Ornelas-Paz, J.d.J.; Ruiz-Cruz, S.; Rios-Velasco, C.; Escalante-Minakata, P. Effect of cultivar on the content of selected phytochemicals in avocado peels. *Food Res. Int.* **2021**, *140*, 110–124. [[CrossRef](#)] [[PubMed](#)]
26. Permal, R.; Chia, T.; Arena, G.; Fleming, C.; Chen, J.; Chen, T.; Chang, W.L.; Seale, B.; Hamid, N.; Kam, R. Converting avocado seeds into a ready to eat snack and analysing for persin and amygdalin. *Food Chem.* **2023**, *399*, 134011. [[CrossRef](#)] [[PubMed](#)]
27. Betiku, E.; Etim, A.O.; Perea, O.; Ojumu, T.V. Two-Step Conversion of Neem (*Azadirachta indica*) Seed Oil into Fatty Methyl Esters Using a Heterogeneous Biomass-Based Catalyst: An Example of Cocoa Pod Husk. *Energy Fuels* **2017**, *31*, 6182–6193. [[CrossRef](#)]
28. Falowo, A.O.; Betiku, E. A novel heterogeneous catalyst synthesis from agrowastes mixture and application in transesterification of yellow oleander-rubber oil: Optimization by Taguchi approach. *Fuel* **2022**, *312*, 122–999. [[CrossRef](#)]
29. Gohain, M.; Laskar, K.; Paul, A.K.; Daimary, N.; Maharana, M.; Goswami, I.K.; Hazarika, A.; Bora, U.; Deka, D. Carica papaya stem: A source of versatile heterogeneous catalyst for biodiesel production and C–C bond formation. *Renew. Energy* **2020**, *147*, 541–555. [[CrossRef](#)]
30. Odude, V.O.; Adesina, A.J.; Oyetunde, O.O.; Adeyemi, O.O.; Ishola, N.B.; Etim, A.; Betiku, E. Application of Agricultural Waste-Based Catalysts to Transesterification of Esterified Palm Kernel Oil into Biodiesel: A Case of Banana Fruit Peel Versus Cocoa Pod Husk. *Waste Biomass Valorization* **2019**, *10*, 877–888. [[CrossRef](#)]

31. Barros, S.D.S.; Pessoa, W.A.G.; Sá, I.S.C.; Takeno, M.L.; Nobre, F.X.; Pinheiro, W.; Manzato, L.; Iglauer, S. Bioresource Technology Pineapple (*Ananás comosus*) leaves ash as a solid base catalyst for biodiesel synthesis. *Bioresour. Technol.* **2020**, *312*, 123–569.
32. Basumatary, S.; Nath, B.; Kalita, P. Application of agro-waste derived materials as heterogeneous base catalysts for biodiesel synthesis. *J. Renew. Sustain. Energy* **2018**, *10*, 043–105. [[CrossRef](#)]
33. Betiku, E.; Okeleye, A.A.; Ishola, N.B.; Osunleke, A.S.; Ojumu, T.V. Development of a Novel Mesoporous Biocatalyst Derived from Kola Nut Pod Husk for Conversion of Kariya Seed Oil to Methyl Esters: A Case of Synthesis, Modeling and Optimization Studies. *Catal. Lett.* **2019**, *149*, 1772–1787. [[CrossRef](#)]
34. Chizoo, E.; Chimamkpan, S.; Gabriel, E.; Gerald, U. Adaptive neuro-fuzzy inference system-genetic algorithm versus response surface methodology-desirability function algorithm modelling and optimization of biodiesel synthesis from waste chicken fat. *J. Taiwan Inst. Chem. Eng.* **2022**, *136*, 104–389.
35. Adepoju, T.F.; Eyibio, U.; Emberru, E.R.; Balogun, T.A. Optimization conversion of beef tallow blend with waste used vegetable oil for fatty acid ethyl ester (FAEE) synthesis in the presence of bio-base derived from Theobroma cacao pod husks. *Case Stud. Chem. Environ. Eng.* **2022**, *6*, 100–218. [[CrossRef](#)]
36. Hasni, K.; Ilham, Z.; Dharna, S.; Varman, M. Optimization of biodiesel production from *Brucea javanica* seeds oil as novel non-edible feedstock using response surface methodology. *Energy Convers. Manag.* **2017**, *149*, 392–400. [[CrossRef](#)]
37. Gohain, M.; Devi, A.; Deka, D. Musa balbisiana Colla peel as highly effective renewable heterogeneous base catalyst for biodiesel production. *Ind. Crops Prod.* **2017**, *109*, 8–18. [[CrossRef](#)]
38. Almeida, V.F.; García-Moreno, P.J.; Guadix, A.; Guadix, E.M. Biodiesel production from mixtures of waste fish oil, palm oil and waste frying oil: Optimization of fuel properties. *Fuel Process. Technol.* **2015**, *133*, 152–160. [[CrossRef](#)]
39. Salim, S.M.; Izriq, R.; Almaky, M.M.; Al-Abbasi, A.A. Synthesis and characterization of ZnO nanoparticles for the production of biodiesel by transesterification: Kinetic and thermodynamic studies. *Fuel* **2022**, *321*, 124–135. [[CrossRef](#)]
40. Yesilyurt, M.K.; Cesur, C.; Aslan, V.; Yilbasi, Z. The production of biodiesel from safflower (*Carthamus tinctorius* L.) oil as a potential feedstock and its usage in compression ignition engine: A comprehensive review. *Renew. Sustain. Energy Rev.* **2020**, *119*, 109–574. [[CrossRef](#)]
41. Giakoumis, E.G.; Sarakatsanis, C.K. Estimation of biodiesel cetane number, density, kinematic viscosity and heating values from its fatty acid weight composition. *Fuel* **2018**, *222*, 574–585. [[CrossRef](#)]

Disclaimer/Publisher’s Note: The statements, opinions and data contained in all publications are solely those of the individual author(s) and contributor(s) and not of MDPI and/or the editor(s). MDPI and/or the editor(s) disclaim responsibility for any injury to people or property resulting from any ideas, methods, instructions or products referred to in the content.